Infrared (broad bands at 2500–3500 cm^{-1}, *vs*) and Raman (2800–3300 cm^{-1}, *w*) spectra suggest that the three-dimensional network of the compound is held together by hydrogen bonding. Unfortunately, the positions of the hydrogen atoms could not be determined and thus the discussion of the hydrogen bonding is necessarily limited and speculative. The following hydrogen-bonding types seem to appear in the structure. (i) All the tellurate oxygen atoms except O(5) carry hydrogen atoms that act as donors to the iodate oxygen atoms [mean O···O distance 2·7 (5) Å]. (ii) The O(4) and O(5^{vii}) atoms are involved in bifurcated hydrogen bonding $O\cdots\begin{matrix}H\\H\end{matrix}\cdots O$. (iii) The O(5) atom can take part only in this type of hydrogen bonding. (iv) The iodate oxygen atoms can act as acceptors for one hydrogen atom [O(7)] or two hydrogen atoms [O(8) and O(9)].

From the point of view of the polar-axis direction, $wR = 0{\cdot}0526$, which corresponds to a structure with the atomic coordinates given in Table 1, is lower than $wR = 0{\cdot}0534$ calculated for the structure with the coordinates related through the centre of inversion, assuming $\alpha = 10^{-6}$ (Rogers, 1981).

References

BOUDJADA, N., BOUDJADA, A. & GUITEL, J. C. (1983). *Acta Cryst.* C**39**, 656–658.

ILJUCHIN, V. V., KALININ, V. R., IVANOVA-KORFINI, I. I. & PACHOMOV, V. I. (1979). *Koord. Khim.* **5**, 1549–1557.

International Tables for X-ray Crystallography (1974). Vol. IV. Birmingham: Kynoch Press.

JOHNSON, C. K. (1965). *ORTEP*. Report ORNL-3794. Oak Ridge National Laboratory, Tennessee.

LINDQVIST, O. (1970). *Acta Chem. Scand.* **24**, 3178–3188.

LINDQVIST, O. (1972). *Acta Chem. Scand.* **26**, 4107–4120.

LOUB, J., HAASE, W. & MERGEHENN, R. (1979). *Acta Cryst.* B**35**, 3039–3041.

MULLICA, D. F., KORP, J. D., MILLIGAN, W. O., BEALL, G. W. & BERNAL, I. (1980). *Acta Cryst.* B**36**, 2565–2570.

ROGERS, D. (1981). *Acta Cryst.* A**37**, 734–741.

SKLENÁŘ, I. (1973). *TLS*. Institute of Physics, Czechoslovak Academy of Sciences, Prague.

WEINLAND, R. F. & PRAUSE, H. (1901). *Z. Anorg. Chem.* **28**, 45–70.

Acta Cryst. (1984). C**40**, 2001–2005

The Structure of γ-Bismuth Molybdate, Bi_2MoO_6, by Powder Neutron Diffraction

BY RAYMOND G. TELLER, JAMES F. BRAZDIL AND ROBERT K. GRASSELLI

Sohio Research Center, 4440 Warrensville Center Road, Cleveland, Ohio 44128, *USA*

AND JAMES D. JORGENSEN

Argonne National Laboratory, Argonne, Illinois 60439, *USA*

(*Received* 7 *February* 1984; *accepted* 30 *August* 1984)

Abstract. $M_r = 609{\cdot}89$, orthorhombic, $Pna2_1$, $a = 5{\cdot}4822$ (3), $b = 16{\cdot}1986$ (8), $c = 5{\cdot}5091$ (3) Å, $V = 489{\cdot}23$ (3) Å^3, $Z = 4$, $D_x = 8{\cdot}28$ g cm^{-3}, $R_p = 0{\cdot}050$. The structure has been determined with room-temperature time-of-flight powder neutron diffraction data. Results of a Rietveld refinement indicate that the structure of the mineral koechlinite, as determined by single-crystal X-ray diffraction, is an adequate representation of the structure of the synthetic material if some adjustments in oxygen-atom positions are made.

Introduction. Bismuth molybdates, Bi_2O_3–$nMoO_3$, have been the subject of intense interest for several decades because they are very selective catalysts for alkene oxidation (Grasselli & Burrington, 1981). As these processes are industrially important, many kinetic and structural studies aimed at elucidating the mechanism of olefin oxidation have been performed. Although too numerous to cite individually, there are several studies that are especially worthy of note: the initial discovery of the activity of these materials for selective oxidation (Veatch, Callahan, Milberger & Foreman, 1960), the realization that lattice oxygen of certain reducible metal oxides can serve as a more versatile and selective oxidizing agent than molecular oxygen for alkene oxidation and ammoxidation, and that the reduced oxides can, in turn, be reoxidized by gaseous oxygen to regenerate the active sites (Callahan & Grasselli, 1963; Callahan, Grasselli, Milberger & Strecker, 1970), mechanistic tracer experiments confirming the pioneering work by Standard Oil (Ohio) workers that the reducible metal oxides themselves are the active catalytic agents (Keulks, 1970; Keulks & Krenzke, 1976) and a number of more recent studies that establish the nature of the intermediate on the catalyst surface (Burrington & Grasselli, 1979) and the importance of catalyst oxidation state which regulates the catalyst activity and selectivity (Brazdil, Suresh & Grasselli, 1980).

0108-2701/84/122001-05$01.50

In the light of the interest in these materials, it is surprising that the structure of the $n = 1$ member of the series is not as yet firmly established. A model based on the single-crystal X-ray structural determination of the mineral koechlinite has been proposed for Bi_2MoO_6 by van den Elzen & Rieck (1973). A problem with this model is that two oxygen atoms come within 2·2 Å of each other (Pertlik & Zemann, 1982), clearly a physically unrealistic feature. Two possible sources for this error are an incorrect model space group for the structure or significant errors in oxygen-atom locations. Either or both of these errors are occasionally found in X-ray structural determinations of high-Z oxide materials, particularly when the metal atoms are at or near high-symmetry positions (as for Bi_2MoO_6). We have therefore collected neutron diffraction data on γ-bismuth molybdate to determine if it and the natural mineral koechlinite have identical structures.

Experimental. γ-Bismuth molybdate was prepared by the coprecipitation method. Stoichiometric amounts of reagent grade (Baker) $(NH_4)_6Mo_7O_{24}$ and $Bi(NO_3)_3$ (in dilute HNO_3) were simultaneously added to a beaker while the solution was rapidly stirred. Because the properties (and perhaps the structure) of Bi_2MoO_6 are altered by minute changes in metal stoichiometry (Matsuura, Shuit & Hirakawa, 1980) the precipitate was not washed. The resultant slurry was stirred and heated to boiling until dry. After drying, the catalyst was heat treated at 563 and 698 K to effect denitrification and then calcined at 823 K for 16 h. The purity of the compound was checked by X-ray diffraction (diffractometer) and Raman scattering. No impurity phases were detected. Time-of-flight neutron diffraction data for Bi_2MoO_6 were collected at the Intense Pulsed Neutron Source (IPNS) on the Special Environment Powder Diffractometer (SEPD) at Argonne National Laboratory. The data were binned in increments of 5 μs. The sample container [seamless vanadium tube approx. $\frac{1}{2}$ in (1·27 cm) in diameter and 4 in (10·16 cm) long] was capped at each end with aluminum plugs. Sample volume was ~5 cm^3 (~10 g). Data were collected at room temperature and atmospheric pressure, no attempt was made to control either temperature or pressure, no precautions were taken against preferred orientation, and no preferred orientation parameters were varied in the refinement. Background was refined simultaneously (5 parameters) with the function $Y = (BK1-BK3-BK5) + (BK2-3BK4)d + (2BK3-8BK5)d^2 + 4BK4d^3 + 8BK5d^4$, where d represents the d spacing. Weights for the profile points are calculated from the expression $[250/I]$ where I is the counter intensity. Absorption corrections were made with the expression $1/[1 + ABSd]$, where ABS is a refinable parameter. All points in the profile that had intensity greater than 0·001 of a maximum peak intensity were considered to have a contribution from that peak. Data below 6000 μs (less than 0·79 Å) were excluded from the analysis. Data from 150° data bank were analyzed with a Rietveld-type profile-fitting program adapted for time-of-flight data. Details of the instrument (Jorgensen & Faber, 1983) and programs used in the analysis (Von Dreele, Jorgensen & Windsor, 1982) have been published. Examination of the raw data revealed two facts: the symmetry of Bi_2MoO_6 is orthorhombic (the 002 and 200 reflections were resolved) and that the cell is primitive. Profile refinement of the data was attempted using three models: (1) atomic parameters were taken from van den Elzen & Rieck's (1973) original X-ray work, space group $Pca2_1$; (2) atomic parameters were generated for a cell with a center of symmetry, $Pbca$, as suggested by Pertlik & Zemann (1982); and (3) atomic parameters as in (2) for space group $Pca2_1$. Refinements 1 and 3 converged to identical results, $R_{prof} = 0·050$, $R_{wprof} = 0·072$, $R_{nucl} = 0·051$ ($R_{exp} = 0·031$); refinement 2 gave a profile agreement factor larger than 1 or 3 by 0·03. Although this does not represent an exhaustive search for the correct model, it encompasses all reasonable models and establishes the most probable space group as $Pca2_1$. In the final cycles of least squares all model parameters (35), a scale factor, background (5), absorption, profile (3) and lattice parameters (3) were refined. For the last cycle max. Δ/σ was 0·10. In addition to positional and thermal (isotropic) parameters, the occupancies of the metal atoms were also refined, for 50 parameters. The values for the occupancies were all within one standard deviation (0·05) of unity. Fig. 1 displays a comparison of observed and calculated profiles. Table 1 gives final atomic parameters for Bi_2MoO_6, and Table 2 lists selected distances and angles. 594 reflections contributed to the profile. Refined cell parameters for γ-bismuth molybdate are $a = 5·4822$ (3), $b = 16·1986$ (8), $c = 5·5091$ (3) Å. X-ray cell constants (van den Elzen & Rieck, 1973) are 5·487 (2), 16·226 (6) and 5·506 (2) Å. Values used for Bi, Mo and O scattering lengths are 0·853, 0·695 and 0·580 respectively (Koester, 1978).*

Discussion. The results of the neutron diffraction refinement confirm that the structure of koechlinite as determined by X-ray diffraction by van den Elzen & Rieck is an adequate representation of synthetic γ-bismuth molybdate. The largest discrepancies between the two structure determinations are in oxygen-atom locations, with the largest involving O(6). In the model derived from the neutron results this atom is

* A list of numerical values for each measured point and experimental details for Bi_2MoO_6 has been deposited with the British Library Lending Division as Supplementary Publication No. SUP 39654 (12 pp.). Copies may be obtained through The Executive Secretary, International Union of Crystallography, 5 Abbey Square, Chester CH1 2HU, England.

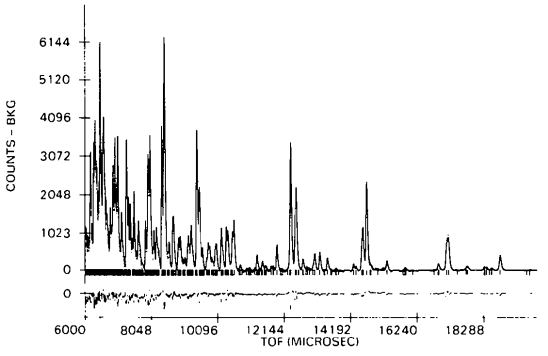

Fig. 1. Plot of observed (points) and calculated (line) neutron diffractograms for Bi_2MoO_6. Marks below the spectra indicate Bragg reflections. A difference curve is presented at the bottom of the plot. Conversion of time-of-flight (TOF) to d spacing is accomplished by the following equation: $TOF = 7567{\cdot}23d - 3{\cdot}01d^2 - 10{\cdot}53$, where TOF is in μs.

Table 1. *Results of the Rietveld refinement of* Bi_2MoO_6

E.s.d.'s in the last digits quoted are given in parentheses.

	x	y	z	B_{iso}(Å^2)
Bi(1)	0·5180 (12)	0·4232 (4)	0·9814 (14)	0·3 (3)
Bi(2)	0·4822 (11)	0·0783 (4)	0·9897 (14)	1·0 (3)
Mo	0·0028 (21)	0·2488 (7)	*0	0·5 (1)
O(1)	0·0556 (19)	0·1407 (8)	0·0959 (20)	0·3 (2)
O(2)	0·2594 (10)	−0·0017 (6)	0·2776 (14)	0·4 (2)
O(3)	0·2360 (13)	0·5006 (8)	0·2664 (22)	1·3 (3)
O(4)	0·6917 (14)	0·2322 (5)	0·2524 (16)	0·9 (2)
O(5)	0·2121 (15)	0·2634 (6)	0·3550 (16)	1·1 (2)
O(6)	0·5654 (22)	0·3589 (10)	0·5700 (19)	1·4 (4)

Occupancies for Bi(1), Bi(2) and Mo were refined to final values of 0·96 (5), 1·05 (5) and 1·00 (3), respectively.

* Not varied in the refinement.

Table 2. *Selected distances* (Å) *and angles* (°) *for* Bi_2MoO_6

The e.s.d.'s for bond lengths and bond angles are 0·01 Å and 0·6°, respectively.

Bi(1)–O(3^{iv})	2·18	Bi(2)–O(1^{ii})	2·40
–O(3^{ii})	2·22	–O(1)	2·61
–O(3^{iii})	2·33	–O(2^{ii})	2·19
–O(3)	2·53	–O(2^{iv})	2·22
–O(6)	2·51	–O(2)	2·38
–O(6^{ii})	2·56	–O(2^{iii})	2·52
–O(5^{ii})	2·96	–O(4)	3·10
Total bond order	2·8		2·8
Mo–O(1)	1·85	O(1)–Mo–O(6^{ii})	151·4
–O(4^{ii})	1·75	O(1)–Mo–O(4)	80·0
–O(4)	2·22	O(1)–Mo–O(4^{ii})	99·9
–O(5^{ii})	1·77	O(1)–Mo–O(5)	77·0
–O(5)	2·28	O(1)–Mo–O(5^{ii})	96·7
–O(6^{ii})	1·86	O(4^{ii})–Mo–O(5)	168·0
Total bond order	5·8	O(4)–Mo–O(5^{ii})	171·9
		O(4^{ii})–Mo–O(6^{ii})	80·3
		O(4)–Mo–O(6^{ii})	100·8
		O(5^{ii})–Mo–O(6^{ii})	79·9
		O(5)–Mo–O(6^{ii})	98·2

Symmetry code: (ii) $\frac{1}{2}-x, y, \frac{1}{2}+z$; (iii) $\frac{1}{2}+x, -y, z$; (iv) $-x, -y, \frac{1}{2}+z$.

located 0·88 Å distant from that of the X-ray model across a pseudo-mirror plane that existed in the X-ray model at $z = \frac{1}{2}$. This movement of O(6) removes the anomalously short O(6)–O(4) distance noted by Pertlik & Zemann and also alters the coordination about Bi(1). The shortest O–O contact distance in the model is 2·59 (1) Å.

The structure of Bi_2MoO_6 consists of layers of corner-sharing MoO_6 octahedra separated by Bi_2O_3 layers. A stereoview of the structure is presented in Fig. 2. There are three types of oxygen atoms in the structure; atoms of the first type [O(4) and O(5)] are within the Mo octahedral layer and bridge only two Mo atoms, total bond orders (Brown & Wu, 1976) about these oxygen atoms are 1·9 and 1·7, respectively [there are also weak interactions between each of these oxygens and Bi atoms, bond lengths are 3·01 (1) and 2·96 (1) Å]. The second type of oxygen is entirely contained within the Bi layer, bridging four metal atoms. The total bond order about these oxygen atoms [O(2) and O(3)] is 2·0 each. Finally, the third type of O atom [O(1) and O(6)] bridges the Mo and Bi layers; they are bonded to one Mo and two Bi atoms each. The total bond orders about these atoms are 1·8 and 1·7 respectively. The bulk oxygen atoms that have the lowest coordination number and lowest bond order should be the most easily removed.

The coordination spheres of the two Bi atoms are nearly identical; Fig. 3 displays oxygens in the first coordination sphere about Bi(1). The oxygen atoms are asymmetrically disposed about the metal atom. This is undoubtedly due to the presence of the Bi lone pair of electrons. Noting the disposition of the coordinating atoms, one can estimate the location of the lone pair, much in the way that hydrogen-atom positions can be inferred in a transition-metal coordination compound by noting the geometry of the ligating non-hydrogen atoms about the central metal atom. This approach is frequently used to locate indirectly hydride ligands in

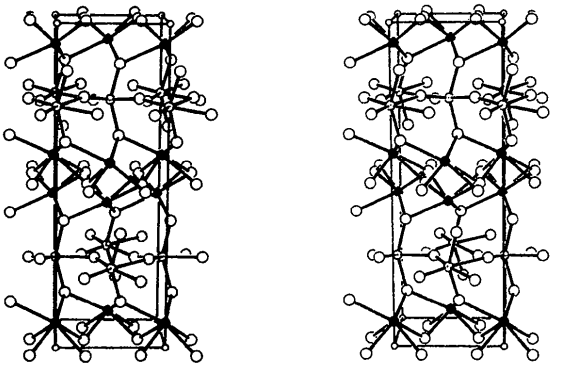

Fig. 2. A stereoscopic view of the unit cell, [100] face. Filled circles represent bismuth atoms, open circles oxygen atoms and dotted circles Mo atoms.

X-ray studies of transition-metal compounds (Teller & Bau, 1979, 1981). A similar situation presents itself here: the asymmetry of the BiO_6 coordination allows one to locate indirectly (and approximately) the lone-electron-pair positions of Bi. Examination of Fig. 2 reveals that each Bi atom directs its lone pair toward the Mo layer. Each MoO_6 octahedron is therefore influenced by two electron pairs from each of the two surrounding Bi layers. Furthermore, the two lone pairs do not approach a given MoO_6 octahedron in a centric manner. In Fig. 2 it can be seen that Bi lone pairs directed upwards appear to bisect the angle formed by the two short Mo–O bonds (or perhaps toward a triangular O_3 face), while Bi electron pairs directed downward are accommodated by octahedral interstices in the corner-sharing MoO_6 layer. The resultant distortion in MoO_6 geometry can be seen in Fig. 4. The six oxygen atoms form an almost perfect octahedron, but the Mo atom is severely displaced toward an O(4)–O(5) pair in the equatorial plane. Examination of the stereoview indicates that the Mo atoms have been distorted approximately toward, rather than away from, the lone pair that bisects the O(4)–Mo–O(5) bond.

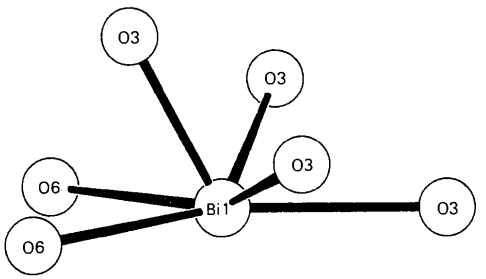

Fig. 3. The first coordination sphere of Bi(1). The asymmetric disposition of the O atoms allows the indirect location of the Bi lone pairs.

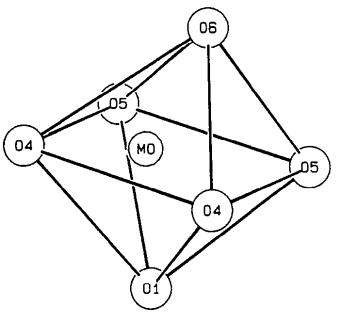

Fig. 4. Coordination about the Mo atom. Note the distortion of the Mo atom within the equatorial plane. The four angles in the equatorial plane are 101·9° between the two short Mo–O bonds, 90·1, 82·1° between the two long Mo–O bonds and 85·9° (e.s.d.'s 0·6°). The Mo atom is displaced from the center of the octahedron in the equatorial plane by 0·30 (1) Å.

Steric considerations would lead one to expect the Mo atoms to be distorted away from this lone electron pair, but the opposite situation appears to occur in Bi_2MoO_6. It is tempting to postulate a Bi lone-pair – Mo atom interaction, just as a Lewis base would interact with a transition metal despite the long Bi···Mo distance (3·8 Å). However, the lack of distortion in the oxygen octahedron eliminates this possibility. A seventh ligand would cause considerable distortion in the O_6 geometry. These considerations lead us to postulate that both Bi lone-pair electrons are directed toward vacant interstices in the MoO_2 layers. Bond-order calculations (see Table 2) about all the metal atoms give results that are each less than that expected for a fully oxidized compound (2·8 *versus* 3·0 for both Bi atoms and 5·8 *versus* 6·0 for Mo). In the only other fully oxidized bismuth molybdate studied with neutron diffraction, $Bi_2Mo_3O_{12}$ (Teller, Brazdil & Grasselli, 1984), bond orders for Mo varied between 5·9 and 6·1 (average = 6·0). Calculated bond orders for Bi were 2·9 and 3·1. This makes the differences between calculated and expected bond orders found in Bi_2MoO_6 marginally significant at best. However, the fact that all calculated values are less than the ideal values invites comment. One obvious explanation for this deviation is partial metal reduction coupled with oxygen deficiency. A small degree of oxygen vacancy would result in an average metal oxidation state of less than 6 and 3 for Mo and Bi, respectively. Hence these calculations indicate that γ-bismuth molybdate may be a nonstoichiometric compound with random oxygen vacancies.

The authors thank the US Department of Energy for supporting IPNS at Argonne as a national users' facility, and the Standard Oil Company (Sohio) for permission to publish this work.

References

BRAZDIL, J. F., SURESH, D. D. & GRASSELLI, R. K. (1980). *J. Catal.* **66**, 347–357.

BROWN, I. D. & WU, K. K. (1976). *Acta Cryst.* B**32**, 1957–1963.

BURRINGTON, J. D. & GRASSELLI, R. K. (1979). *J. Catal.* **59**, 79–90.

CALLAHAN, J. L. & GRASSELLI, R. K. (1963). *Am. Inst. Chem. Eng. J.* **9**, 755–757.

CALLAHAN, J. L., GRASSELLI, R. K., MILBERGER, E. C. & STRECKER, H. A. (1970). *Ind. Eng. Chem. Prod. Res. Dev.* **9**, 134–144.

ELZEN, A. F. VAN DEN & RIECK, G. D. (1973). *Acta Cryst.* B**29**, 2436–2439.

GRASSELLI, R. K. & BURRINGTON, J. D. (1981). *Adv. Catal.* **30**, 133–141.

JORGENSEN, J. D. & FABER, J. (1983). ICANS-II. Proc. VIth Int. Collaboration on Advanced Neutron Sources. Report ANL-82-80. Argonne National Laboratory, Illinois.

KEULKS, G. W. (1970). *J. Catal.* **19**, 232–238.

KEULKS, G. W. & KRENZKE, D. L. (1976). 6th Int. Congress on Catalysis, London, pp. 806–820.

KOESTER, L. (1978). *Neutron Physics.* In *Springer Tracts in Modern Physics*, Vol. 80, pp. 34–41. Berlin: Springer.
MATSUURA, I., SHUIT, R. & HIRAKAWA, K. (1980). *J. Catal.* **63**, 152–164.
PERTLIK, F. & ZEMANN, J. (1982). *Fortschr. Mineral. Beih.* **60**(1), 162–163.
TELLER, R. G. & BAU, R. (1979). *Acc. Chem. Res.* **12**, 176–188, and references cited therein.
TELLER, R. G. & BAU, R. (1981). *Struct. Bonding (Berlin)*, **44**, 1–48.
TELLER, R. G., BRAZDIL, J. B. & GRASSELLI, R. K. (1984). In preparation.
VEATCH, F., CALLAHAN, J. L., MILBERGER, E. C. & FOREMAN, R. M. (1960). Proc. 2nd Catalysis Conference, Paris.
VON DREELE, R. B., JORGENSEN, J. D. & WINDSOR, C. G. (1982). *J. Appl. Cryst.* **15**, 581–590.

Acta Cryst. (1984). C**40**, 2005–2006

phyllo-Nonafluoropentazinn(II)-tetrafluoroborat, $[Sn_5F_9][BF_4]$

VON JOHANNES BÖNISCH UND GÜNTER BERGERHOFF

Anorganisch-chemisches Institut, Universität Bonn, Gerhard-Domagk-Strasse 1, *D*-5300 *Bonn* 1, *Bundesrepublik Deutschland*

(*Eingegangen am* 26. *März* 1984; *angenommen am* 29. *August* 1984)

Abstract. $M_r = 851{\cdot}2$, monoclinic, $P2_1/c$, $a = 13{\cdot}635\ (2)$, $b = 7{\cdot}660\ (2)$, $c = 14{\cdot}112\ (2)$ Å, $\beta = 119{\cdot}71\ (1)°$, $V = 1280{\cdot}04$ Å^3, $Z = 4$, $D_x = 4{\cdot}42$ g cm^{-3}, $\lambda(\text{Mo } K\alpha) = 0{\cdot}71069$ Å, $\mu(\text{Mo } K\alpha) = 98{\cdot}14$ cm^{-1}, $F(000) = 1488$, room temperature, $R = 0{\cdot}077$, 3715 unique reflections. The structure of the synthetic compound consists of two-dimensional nets, built up by three- and four-connected SnF_3 and SnF_4 pyramids with BF_4 groups between the nets.

Einleitung. In nichtwässrigen Lösungsmitteln kann das tetramere $(SnF_2)_4$ (McDonald, Ho-Kuen Hau & Eriks, 1976) durch Entzug von F^--Ionen zu polymeren Kationen abgebaut werden. In Acetonitril entstehen aus SnF_2 mit Bortrifluorid der Reihe nach die Verbindungen $Sn_2F_3BF_4$, $Sn_3F_5BF_4$, $Sn_5F_9BF_4$ und sicher eine weitere (Bönisch & Bergerhoff, 1981).

Experimentelles. Erhitzt man ein Gemisch aus Zinn(II)-fluorid, Bortrifluorid–methylätherat und Acetonitril im Molverhältnis 1:10:9 zum Sieden, so entsteht eine klare Lösung, aus der beim Abkühlen Kristalle von $Sn_2F_3BF_4$ ausfallen. Mit 13 molaren Teilen Wasser lösen sich diese wieder und auf Zugabe von 17 molaren Teilen Diäthyläther entstehen aus der Lösung langsam Einkristalle. Sie wurden früher (Bönisch & Bergerhoff, 1981) auf Grund von ^{19}F-Kernresonanzmessungen als $Sn_4F_7BF_4$ angesprochen. Die damals gefundene Zelle (1) lässt sich über die Vektorgleichungen $\mathbf{a}_2 = \mathbf{a}_1$, $\mathbf{b}_2 = \mathbf{c}_1$, $\mathbf{c}_2 = -\frac{1}{2}\mathbf{a}_1 - \frac{1}{2}\mathbf{b}_1$ in die im *Abstract* genannte Zelle (2) überführen. Die Strukturbestimmung erweist die Verbindung als $Sn_5F_9BF_4$.

Auf einem Nonius-CAD-4-Diffraktometer wurden an einem Kristall der Grösse 0,3 × 0,25 × 0,06 mm die Gitterkonstanten aus 25 Reflexen zwischen $2\theta = 7{,}7$ und 17,6° bestimmt und die Intensitäten von 12 911 Reflexen im Bereich $5{,}8 < 2\theta < 59{,}9°$ gemessen (*hkl*: −19,0,−19 bis 19,10,19). Von den 3715 nichtäquivalenten Reflexen waren 2060 mit $I < 3{,}3\sigma(I)$ als so schwach einzustufen, dass ihre Intensitäten nicht mit der gleichen hohen Reproduzierbarkeit gemessen wurden wie die stärkeren. Für Absorption wurde nicht korrigiert. Standardreflexe zeigten keine Intensitätsschwankungen. Die Zinn-Atome liessen sich durch direkte Methoden ermitteln (Main, Hull, Lessinger, Germain, Declercq & Woolfson, 1978), die an Zinn gebundenen Fluor-Atome wurden durch sukzessive Verfeinerungs- und Fouriersynthesecyclen (Stewart, Machin, Dickinson, Ammon, Heck & Flack, 1976) festgelegt. Die BF_4-Gruppe liess sich erst über eine Differenzfouriersynthese lokalisieren. Die Atomstreufaktoren wurden nach Cromer & Mann (1968) hergeleitet. Die bei der abschliessenden Verfeinerungsrechnung nach der Methode der kleinsten Quadrate unter Benutzung der Strukturamplituden F mit anisotropen Temperaturfaktoren erhaltenen Koordinaten zeigt Tabelle 1.* $w = 1/\sigma^2(F)$, $(\Delta/\sigma)_{max} = 0{,}15$. Keine Korrektur für sekundäre Extinktion.

Diskussion. Fig. 1 zeigt ein Stereobild der Struktur in Blickrichtung [010], bei dem Sn—F-Abstände < 2,5 Å eingezeichnet sind. In Verbindung mit Tabelle 2 erkennt man, dass die Zinn-Atome an der Spitze von Pyramiden sitzen, die über alle ihre Fluor-Atome zu einem zweidimensionalen Netz in der (100) Ebene verknüpft sind. Mit einem mittleren F—Sn—F-Winkel von 83° bei den dreiseitigen Pyramiden, einem grossen (142°) und einem kleinen (81°) Winkel bei den

* Die Liste der Strukturfaktoren und die Tabelle der anisotropen Temperaturfaktoren sind bei der British Library Lending Division (Supplementary Publication No. SUP 39703: 34 pp.) hinterlegt. Kopien sind erhältlich durch: The Executive Secretary, International Union of Crystallography, 5 Abbey Square, Chester CH1 2HU, England.

0108-2701/84/122005-02$01.50